JOURNAL OF COMPUTATIONAL PHYSICS **80**, 314–330 (1989)

Spectral Collocation Methods for Stokes Flow in Contraction Geometries and Unbounded Domains

A. KARAGEORGHIS AND T. N. PHILLIPS

Department of Mathematics, University College of Wales, Aberystwyth SY23 3BZ, United Kingdom

Received July 24, 1987; revised March 22, 1988

A spectral element method is described which enables Stokes flow in contraction geometries and unbounded domains to be solved as a set of coupled problems over semi-infinite rectangular subregions. Expansions in terms of the eigenfunctions of singular Sturm–Liouville problems are used to compute solutions to the governing biharmonic equation for the stream function. The coefficients in these expansions are determined by collocating the differential equation and boundary conditions and imposing C^3 continuity across the subregion interface. The suitability of domain truncation and algebraic mapping techniques are compared as well as the choice of trial functions. © 1989 Academic Press, Inc.

1. INTRODUCTION

In this paper we investigate techniques for numerically solving Stokes flow in a contraction, i.e., an infinite channel whose diameter changes abruptly. The numerical solution of such problems in unbounded domains involves two approximations. First, the solution must be approximated by some representation. The unknowns in such a representation are determined by satisfying the differential equation and boundary conditions, in some sense. Second, the unbounded domain may be approximated by a finite domain. We are particularly interested in the effect upon the solution of the treatment of the unbounded domain.

In the study of non-Newtonian fluids through tortuous geometries it is well known that the behaviour of the flow is dependent on the entry and exit lengths [4]. The entry length needs to be increased as the elasticity parameter, or Weissenberg number, increases so that a fully developed velocity profile can be imposed in the entry and exit sections. When such problems are solved numerically this places a limitation on the value of the Weissenberg number for which computations are practicable. The need to overcome this restriction provides the motivation for the current study, i.e., our ultimate aim is to solve the equations governing the flow of a non-Newtonian fluid with no limitation on the Weissenberg number using techniques developed in this paper for treating unbounded domains.

Grosch and Orszag [10] studied the problem of solving ordinary differential equations in unbounded regions using Chebyshev polynomials. Since the

0021-9991/89 $3.00

Chebyshev polynomials are defined on a finite interval they proposed two procedures to overcome this difficulty. The most obvious one, known as domain truncation, imposes an artificial boundary condition at a large but finite distance. The problem is then solved in the finite region. The second procedure solves the problem in a transformed region. This is achieved by mapping the semi-infinite region $0 \leqslant x < \infty$, for example, onto the finite region $0 \leqslant z \leqslant 1$ using either an algebraic mapping of the form

$$z = \frac{x}{x + L}$$

or an exponential mapping of the form

$$z = 1 - e^{-x/L},$$

where the parameter L is known as the mapping factor. The outcome of their work was that if the exact solution to the differential equation decayed exponentially fast as $|x| \rightarrow \infty$, then all the methods would work but the use of the algebraic mapping produced the best results. However, if the solution oscillates at infinity then the mappings fail.

Using the method of steepest descents, Boyd [1] compared the effectiveness of these methods for solving problems in a semi-infinite or infinite domain using Chebyshev polynomials. Boyd used these methods to obtain approximations to known functions and not to find solutions to differential equations. He also gives estimates of the optimum choice of domain size or mapping factor.

The study of the numerical simulation of non-Newtonian fluids has generated much interest in recent years. At the present time finite element methods enjoy a high level of popularity and success in the field due mainly to their flexibility which facilitates the numerical solution of problems defined in general, irregular regions. One of the remaining problems of major importance in the simulation of such flows is the so-called high Weissenberg number problem. This concerns the breakdown of convergence of a method or degradation of numerical solutions as the Weissenberg number is increased. Marchal and Crochet [16] have shown that in a mixed finite element formulation this problem can be avoided for larger values of the Weissenberg number if higher order (Hermitian) trial functions are used. We plan to take this idea a step further by considering spectral methods which, by definition, use high order global trial functions.

The governing equations in non-Newtonian fluid mechanics consist of field equations and constitutive equations. The field equations comprise the equation of continuity, the conservation of momentum, and the local expression of the principle of balance of angular momentum. For the plane, inertialess flow of an incompressible fluid these statements assume the mathematical form

$$\nabla \cdot \mathbf{v} = 0, \tag{1.1}$$

$$\nabla \cdot \mathbf{P} = 0, \tag{1.2}$$

where $\mathbf{v}$ denotes the velocity field and $\mathbf{P}$ the Cauchy stress tensor. The principle of balance of angular momentum in the absence of body and surface couples requires that the Cauchy stress tensor $\mathbf{P}$ be symmetric.

The constitutive equation for a corotational Maxwell model is given by

$$\mathbf{T} + \lambda \mathring{\mathbf{T}} = 2\eta \mathbf{D}, \tag{1.3}$$

where $\mathbf{D}$ is the rate of deformation tensor, $\mathbf{T}$ the extra-stress tensor, and λ and η are material constants. For an incompressible fluid, the motion of the continuum determines the stress tensor up to an arbitrary isotropic tensor and thus $\mathbf{P}$ and $\mathbf{T}$ are related as

$$\mathbf{P} = -p\mathbf{I} + \mathbf{T}, \tag{1.4}$$

where p is an arbitrary pressure and $\mathbf{I}$ the identity tensor. The corotational derivative $\mathring{\mathbf{T}}$ is an average of the upper and lower convected derivatives.

The introduction of a stream function ψ, defined by

$$u = \frac{\partial \psi}{\partial y}, \qquad v = -\frac{\partial \psi}{\partial x}, \tag{1.5}$$

means that Eq. (1.1) is automatically satisfied. Further, the stress field $\mathbf{P}$ may be represented in terms of an Airy stress function χ (scalar) as

$$P_{11} = \frac{\partial^2 \chi}{\partial y^2}, \qquad P_{22} = \frac{\partial^2 \chi}{\partial x^2}, \qquad P_{12} = -\frac{\partial^2 \chi}{\partial x\, \partial y}. \tag{1.6}$$

This representation ensures the satisfaction of Eq. (1.2). The only differential equation that is not already satisfied is therefore the constitutive equation (1.3). This equation may be written in terms of the scalar functions ψ, χ, and p yielding three scalar differential equations in terms of these variables. Coleman [2, 3] eliminates the pressure and, by defining a complex potential ϕ to be $\chi + 2i\eta\psi$, shows that the governing equation for the creeping flow of a corotational Maxwell fluid may be written in the form

$$\frac{\partial^2 \phi}{\partial \bar{z}^2} + \frac{i\lambda}{\eta}\left[\frac{\partial \operatorname{Im} \phi}{\partial \bar{z}} \frac{\partial}{\partial z} - \frac{\partial \operatorname{Im} \phi}{\partial z} \frac{\partial}{\partial \bar{z}} - 2\frac{\partial^2 \operatorname{Im} \phi}{\partial z\, \partial \bar{z}}\right] \frac{\partial^2 \operatorname{Re} \phi}{\partial \bar{z}^2} = 0. \tag{1.7}$$

This equation may be written in terms of the real variables ψ and χ and manipulated to obtain the coupled system

$$\nabla^4 \psi = WA(\partial^2\psi, \partial^3\psi, \partial^4\psi, \partial^2\chi, \partial^3\chi, \partial^4\chi), \tag{1.8a}$$

$$(1 + W\mathbf{v} \cdot \nabla)\, \nabla^4 \chi = WB(\partial^2\psi, \partial^3\psi, \partial^4\psi, \partial^2\chi, \partial^3\chi, \partial^4\chi), \tag{1.8b}$$

where A and B are bilinear forms in their arguments, and ∂ denotes partial differentiation with respect to x or y. The Weissenberg number, W, is an elasticity parameter and is a measure of the fluid's memory.

The success of spectral methods in solving the *primary* problem, which is a one-dimensional model of (1.8b), has already been demonstrated [6, 13]. Plane creeping Newtonian flow may be described using a stream function that satisfies a biharmonic equation. This type of flow is also known as Stokes flow. If we are to have a realistic chance of solving (1.8) then spectral element techniques need to be developed for solving these equations in unbounded domains. This is the subject that the present paper addresses for Stokes flow which is the simplest form of (1.8a) with $W=0$.

Consider Stokes flow through a $1:\alpha$ contraction depicted in Fig. 1. In terms of the stream function $\psi(x, y)$ the governing equations may be recast in the single equation

$$\nabla^4\psi = 0, \tag{1.9}$$

where ∇^4 is the biharmonic operator. The introduction of the stream function effectively means that the continuity equation is automatically satisfied. An advantage of this formulation over the stream function–vorticity formulation is that we do not need to manufacture boundary conditions for the vorticity. We note that the x-axis represents an axis of symmetry for the problem.

We solve Eq. (1.9) subject to the following boundary conditions on $\psi(x, y)$:

$$\psi(x, 1) = 1, \qquad \frac{\partial\psi}{\partial y}(x, 1) = 0, \qquad -\infty < x \leqslant 0, \tag{1.10}$$

$$\psi(0, y) = 1, \qquad \frac{\partial\psi}{\partial x}(0, y) = 0, \qquad \alpha \leqslant y \leqslant 1, \tag{1.11}$$

$$\psi(x, \alpha) = 1, \qquad \frac{\partial\psi}{\partial y}(x, \alpha) = 0, \qquad 0 \leqslant x < \infty, \tag{1.12}$$

$$\psi(x, 0) = 0, \qquad \frac{\partial^2\psi}{\partial y^2}(x, 0) = 0, \qquad -\infty < x < \infty, \tag{1.13}$$

$$\psi(x, y) \to G_{\mathrm{I}}(y) \quad \text{as} \quad x \to -\infty, \qquad 0 \leqslant y \leqslant 1, \tag{1.14}$$

$$\psi(x, y) \to G_{\mathrm{II}}(y) \quad \text{as} \quad x \to \infty, \qquad 0 \leqslant y \leqslant \alpha, \tag{1.15}$$

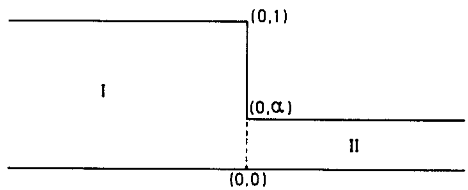

FIG. 1. Contraction geometry.

where

$$G_{\mathrm{I}}(y)=\tfrac{1}{2}y(3-y^2), \qquad G_{\mathrm{II}}(y)=G_{\mathrm{I}}(y/\alpha).$$

The region of interest is divided into two semi-infinite rectangular subregions as shown in Fig. 1. Other possibilities exist for decomposing the flow region, for example, the use of three elements with a triple point at $(0, \alpha)$. We feel that there is no strong justification in using a larger number of elements, since this would complicate the implementation considerably. Within each of these subregions we represent the solution of Eq. (1.9) in the form of a truncated series involving orthogonal polynomials. A discussion about the choice of orthogonal polynomials is given later. The unknown coefficients in these expansions are determined by satisfying the differential equation (1.9) and boundary conditions (1.10)–(1.15) at selected points in the region (collocation points) and the solutions in the two subregions are matched by imposing continuity conditions across the interface. This is the essence of the spectral element method reported here. The earlier work of Patera [21] and Phillips and Davies [22] on spectral element methods uses a Galerkin formulation to determine the expansion coefficients. Other global decomposition techniques have appeared previously in the solution of boundary value problems and in computational fluid dynamics [9, 7, 19]. The main differences between these techniques lie in the choice of trial functions and in the treatment of the continuity conditions at element interfaces. In this work a collocation approach is favoured over a variational formulation since although a variational principle exists for the biharmonic equation, no such simple principle exists for the Navier–Stokes equations [24] or the equations governing non-Newtonian flow. It should be pointed out, however, that in situations like these a variational form in the sense of a weak, integrated-by-parts form can be used and has the advantage of reducing the regularity and continuity requirements of the trial space.

The Stokes poblem under consideration has a singularity at the re-entrant corner $(0, \alpha)$ which has been the subject of several studies [18, 11]. Phillips and Davies [22] treat the re-entrant corner singularity for the Poisson problem using a post-processing technique in conjunction with a two-element discretization of the 4:1 contraction geometry. Using this procedure, they obtain accurate solutions in the locality of the singularity. Such a technique can also be applied to this problem using the asymptotic expansion of the singularity derived by Moffatt [18]. Some progress in obtaining an asymptotic form for the non-Newtonian case is being made [5].

2. The Choice of Trial Functions in Spectral Methods

In a spectral method the solution to a differential equation is represented by means of a truncated series of smooth, global functions. If the eigenfunctions of singular Sturm–Liouville problems are chosen as trial functions then for linear problems with smooth solutions this choice yields expansions which can converge asymptotically faster than any finite power of N^{-1}. If the eigenfunctions of a related but simpler differential operator to that in the equation to be solved are used then exponential convergence is only observed when the problem possesses special properties. A comparison of the merits of these choices for solving a nonlinear problem is given in Davies, Karageorghis, and Phillips [6]. They show that as for linear problems the rapid rate of convergence is maintained when Chebyshev polynomials are used as trial functions, and that this choice is not sensitive to the level of nonlinearity. Joseph [12] obtained solutions for the slow flow over a rectangular slot by matching biorthogonal eigenfunction expansions in different regions of the flow. The expansions are in terms of the eigenfunctions of the biharmonic operator and are known as the Papkovich–Fadle eigenfunctions. The work of Davies, Karageorghis, and Phillips [6] on one-dimensional nonlinear problems supports the use of Chebyshev polynomials over beam functions, which are the one-dimensional analog of Papkovich–Fadle eigenfunctions. Therefore, since our ultimate aim is to solve highly nonlinear differential equations, we only consider the eigenfunctions of singular Sturm–Liouville problems as trial functions. In particular, we investigate the performance of Chebyshev and Laguerre polynomials.

The spectral collocation method is used to determine the numerical coefficients in the truncated series expansion. In this method the test functions are translated Dirac delta functions which means that the differential equation is satisfied exactly at a selected set of collocation points. Collocation is chosen in preference to Galerkin since the algebraic system for the expansion coefficients is then easier to formulate, although if numerical quadrature is used to evaluate the integrals which appear in a variational form then an essentially collocation scheme results.

Spectral methods possess approximation properties superior to finite difference and finite element methods for problems in which the solution is smooth. The advantage of finite element methods is their ability to treat complex geometries. The spectral element method introduced by Patera [21] seeks to combine the advantages of both the spectral and finite element methods. The contraction geometry is therefore divided into two semi-infinite rectangular elements shown in Fig. 1 and a spectral approximation to the solution of Eq. (1.9) is sought within each constituent rectangle. We approximate the stream function $\psi(x, y)$ by $\psi_{\mathrm{I}}(x, y)$ in region I and $\psi_{\mathrm{II}}(x, y)$ in region II, where

$$\psi_{\mathrm{I}}(x, y) = G_{\mathrm{I}}(y) + \sum_{m=0}^{M} \sum_{n=0}^{N} a_{mn} f_m^{\mathrm{I}}(x)\, g_n^{\mathrm{I}}(y), \tag{2.1}$$

$$\psi_{\mathrm{II}}(x, y) = G_{\mathrm{II}}(y) + \sum_{m=0}^{L} \sum_{n=0}^{N} b_{mn} f_m^{\mathrm{II}}(x)\, g_n^{\mathrm{II}}(y), \tag{2.2}$$

and $f_m^{\mathrm{I}}(x)$, $f_l^{\mathrm{II}}(x)$ $(0 \leqslant m \leqslant M,\ 0 \leqslant l \leqslant L)$ and $g_n^{\mathrm{I}}(y)$, $g_n^{\mathrm{II}}(y)$ $(0 \leqslant n \leqslant N)$ are appropriately chosen trial functions in the x- and y-directions, respectively.

We consider the following three choices of trial functions in (2.1) and (2.2):

(a) Chebyshev–Laguerre representation in the original domain;
(b) Chebyshev–Chebyshev representation in a truncated domain;
(c) Chebyshev–Chebyshev representation in a mapped domain.

The choice in (a) uses modified Chebyshev polynomials in the y-direction and weighted Laguerre polynomials in the x-direction. The Laguerre polynomials are weighted with a decaying exponential function to ensure that

$$f^{\rm I}_m(x) \to 0 \text{ as } x \to -\infty, \qquad f^{\rm II}_l(x) \to 0 \text{ as } x \to \infty,$$

for $0 \leqslant m \leqslant M$, $0 \leqslant l \leqslant L$. For choice (b) the domain is truncated at a finite distance from the interface which effectively means that given entry and exit lengths are imposed. A double Chebyshev representation is used in each truncated subregion to approximate the stream function. The last approach maps each of the semi-infinite subregions onto a finite rectangle using an algebraic mapping in the x-direction. A double Chebyshev representation is then sought in the mapped domain.

3. Spectral Collocation Strategy

In order to have a complete description of the solution we need to determine the unknown expansion coefficients appearing in the spectral approximations (2.1) and (2.2). There are a total of $(M+L+2)(N+1)$ coefficients to be calculated. These are found by collocating the differential equation, boundary conditions, and interface continuity conditions. Some of the boundary conditions are automatically satisfied by the particular choice of trial functions used, whereas others are to be satisfied approximately using collocation.

In region I we consider the set of collocation points

$$S_1 = \{(x^{\rm I}_i, y^{\rm I}_j)\colon 0 \leqslant i \leqslant M,\ 0 \leqslant j \leqslant N,\ x^{\rm I}_M = 0,\ y^{\rm I}_0 = 0,\ y^{\rm I}_N = 1\},$$

and in region II the set of points

$$S_2 = \{(x^{\rm II}_i, y^{\rm II}_j)\colon 0 \leqslant i \leqslant L, 0 \leqslant j \leqslant N, x^{\rm II}_0 = 0,\ y^{\rm II}_0 = 0,\ y^{\rm II}_N = \alpha\}.$$

The coefficients a_{mn} and b_{mn} are chosen to satisfy (1.9) exactly at a set of collocation points $T_1 \subset S_1$ in region I and $T_2 \subset S_2$ in region II. Substitution of (2.1) and (2.2) into (1.9) yields the linear equations

$$\nabla^4 \psi_{\rm I} = 0, \qquad \text{for} \quad (x, y) \in T_1, \tag{3.1}$$

$$\nabla^4 \psi_{\rm II} = 0, \qquad \text{for} \quad (x, y) \in T_2. \tag{3.2}$$

In addition we apply C^0 and C^1 continuity across the interface $x = 0$, $0 \leqslant y \leqslant 1$ at the set of collocation points $T_3 \subset S_1$ and C^2 and C^3 continuity across the interface

$x=0$, $0 \leqslant y \leqslant \alpha$ at the collocation points $T_4 \subset S_2$ These requirements lead to the linear equations

$$\psi_{\mathrm{I}}(0, y)=\begin{cases}\psi_{\mathrm{II}}(0, y), & \text{if } (0, y) \in T_3 \text{ and } 0 \leqslant y \leqslant \alpha, \\ 1, & \text{if } (0, y) \in T_3 \text{ and } \alpha \leqslant y \leqslant 1,\end{cases} \tag{3.3}$$

$$\frac{\partial \psi_{\mathrm{I}}}{\partial x}(0, y)=\begin{cases}\dfrac{\partial \psi_{\mathrm{II}}}{\partial x}(0, y), & \text{if } (0, y) \in T_3 \text{ and } 0 \leqslant y \leqslant \alpha, \\ 0, & \text{if } (0, y) \in T_3 \text{ and } \alpha \leqslant y \leqslant 1,\end{cases} \tag{3.4}$$

$$\frac{\partial^2 \psi_{\mathrm{I}}}{\partial x^2}(0, y)=\frac{\partial^2 \psi_{\mathrm{II}}}{\partial x^2}(0, y), \quad \text{if } (0, y) \in T_4 \text{ and } 0 \leqslant y \leqslant \alpha, \tag{3.5}$$

$$\frac{\partial^3 \psi_{\mathrm{I}}}{\partial x^3}(0, y)=\frac{\partial^3 \psi_{\mathrm{II}}}{\partial x^3}(0, y), \quad \text{if } (0, y) \in T_4 \text{ and } 0 \leqslant y \leqslant \alpha. \tag{3.6}$$

When all the other boundary conditions are satisfied, the sets T_1, T_2, T_3, and T_4 are chosen in the following way in order to obtain the same number of equations as unknowns:

$$T_1=\{(x_i^{\mathrm{I}}, y_j^{\mathrm{I}}): 0 \leqslant i \leqslant M-2, 2 \leqslant j \leqslant N-2\} \tag{3.7}$$

$$T_2=\{(x_i^{\mathrm{II}}, y_j^{\mathrm{II}}): 3 \leqslant i \leqslant L, 2 \leqslant j \leqslant N-2\}, \tag{3.8}$$

$$T_3=\{(0, y_j^{\mathrm{I}}): 2 \leqslant j \leqslant N-2\}, \tag{3.9}$$

$$T_4=\{(0, y_j^{\mathrm{II}}): 2 \leqslant j \leqslant N-2\}. \tag{3.10}$$

The omission of the extreme collocation points in S_1 and S_2 means that near the boundaries and the subregion interface the approximations ψ_{I} and ψ_{II} are influenced more by the boundary conditions and interface continuity conditions than by the differential equation. When some of the boundary conditions remain to be satisfied then the sets T_1 and T_2 are modified in a way described later.

The resulting system of linear equations obtained by collocation as described above is solved using a Crout factorization technique from the NAG Library. This requires $O[(M+L+2)^3(N+1)^3]$ operations.

4. Spectral Discretization

4.1. *Chebyshev–Laguerre in Original Domain*

In this appoach, modified Chebyshev polynomials are used in the y-direction and weighted Laguerre polynomials in the x-direction. For the representation (2.1) in region I, for example, we take

$$f_m^{\mathrm{I}}(x)=e^{b_{\mathrm{I}} x} L_m(-x), \tag{4.1}$$

$$g_n^{\mathrm{I}}(y)=P_n(y), \tag{4.2}$$

where

$$L_m(x) = \sum_{k=0}^{m} \frac{(-1)^k}{k!} c_k^m x^k, \tag{4.3}$$

are the Laguerre polynomials (see [23]) and

$$P_n(y) = T_n^*(y) + \alpha_n T_3^*(y) + \beta_n T_2^*(y) + \gamma_n T_1^*(y) + \delta_n T_0^*(y) \tag{4.4}$$

are the modified Chebyshev polynomials with $T_n^*(y)$ defined by

$$T_n^*(y) = T_n(2y-1) = \cos(n \cos^{-1}(2y-1)). \tag{4.5}$$

The constant $b_{\rm I}$ in (4.1) is a parameter to be chosen. It represents the rate of decay of the solution as $x \to -\infty$. This motivated our choice of $b_{\rm I}$ to be the real part of the principal Papkovich–Fadle eigenvalue. The constants $\alpha_n, \beta_n, \gamma_n$, and δ_n are constants chosen so that (2.1) satisfies the boundary conditions (1.10) and (1.13) in region I. These boundary conditions are automatically satisfied if

$$\begin{aligned}
\alpha_n &= \tfrac{1}{32}\{-n^2 - \tfrac{1}{2}(-1+(-1)^n) + \tfrac{1}{3}(-1)^n n^2(n^2-1)\},\\
\beta_n &= 6\alpha_n - \tfrac{1}{12}(-1)^n n^2(n^2-1),\\
\gamma_n &= -\alpha_n + \tfrac{1}{2}(-1+(-1)^n),\\
\delta_n &= -1 - \alpha_n - \beta_n - \gamma_n.
\end{aligned} \tag{4.6}$$

Following the recommendations of Orszag [20] we choose the collocation points in the y-direction to be the extrema of the Chebyshev polynomial of highest degree used in the solution representations. It is known that this choice gives rise to optimal approximation properties of smooth functions. We therefore take

$$y_j^{\rm I} = \frac{1}{2}\left\{1 + \cos \pi \left(1 - \frac{j}{N}\right)\right\} \tag{4.7}$$

and

$$y_j^{\rm II} = \frac{1}{2}\alpha\left\{1 + \cos \pi \left(1 - \frac{j}{N}\right)\right\}. \tag{4.8}$$

The choice of collocation points in a Laguerre method and the theoretical justification of the resulting numerical techniques are contained in a paper by Maday *et al.* [14]. Mivriplis [15] uses Gauss–Radau type Laguerre quadrature to accurately evaluate the integrals which appear in a variational form of the one-dimensional Helmholtz equation defined on a semi-infinite interval. In the same spirit as the choice of collocation points in the y-direction we consider the zeros or extrema of the weighted Laguerre polynomial of highest degree as collocation points in the x-direction.

4.2. *Chebyshev–Chebyshev in Truncated Domain*

Here the domain is truncated at a distance h_1 from the interface in region I and at a distance h_2 from the interface in region II. For the representation (2.1) in region I, for example, we take

$$f_m^{\mathrm{I}}(x) = T_m^{h_1}(x),$$
$$g_n^{\mathrm{I}}(y) = P_n(y),$$

where $T_m^{h_1}(x)$ is the Chebyshev polynomial defined on the interval $[-h_1, 0]$ by

$$T_m^{h_1}(x) = T_m\left(\frac{2x}{h_1} + 1\right),$$

and $P_n(y)$ are the modified Chebyshev polynomials defined in the previous section. The collocation points are chosen to be the extrema of the Chebyshev polynomial defined on the appropriate interval.

Since the domain is truncated, fictitious boundary conditions need to be imposed along the entry and exit sections. Therefore we apply the boundary conditions:

$$\psi_{\mathrm{I}}(-h_1, y) = G_{\mathrm{I}}(y), \qquad \frac{\partial \psi_{\mathrm{I}}}{\partial x}(-h_1, 0) = 0, \qquad 0 \leqslant y \leqslant 1, \tag{4.9}$$

$$\psi_{\mathrm{II}}(h_2, y) = G_{\mathrm{II}}(y), \qquad \frac{\partial \psi_{\mathrm{II}}}{\partial x}(h_2, y) = 0, \qquad 0 \leqslant y \leqslant \alpha. \tag{4.10}$$

These boundary conditions assume a fully developed velocity profile at the inflow $x = -h_1$ and at the outflow $x = h_2$. The choice of h_1 and h_2 is discussed in the numerical results section.

4.3. *Chebyshev–Chebyshev in Mapped Domain*

In this section we extend the work of Grosch and Orszag [10] to differential equations defined in two space dimensions. The subregions I and II are each mapped into a finite rectangle by means of an algebraic mapping. If we define subregion I by the set of points

$$R_{\mathrm{I}} = \{(x, y)\colon -\infty < x \leqslant 0, 0 \leqslant y \leqslant 1\},$$

then under the algebraic mapping

$$z = \frac{x}{x + L_{\mathrm{I}}}, \qquad L_{\mathrm{I}} < 0, \tag{4.11}$$

R_{I} is mapped onto M_{I}, where

$$M_{\mathrm{I}} = \{(z, y)\colon 0 \leqslant z \leqslant 1, 0 \leqslant y \leqslant 1\}.$$

Similarly, subregion II is mapped onto M_{II}, where

$$M_{\mathrm{II}} = \{(z, y): 0 \leqslant z \leqslant 1, 0 \leqslant y \leqslant \alpha\}$$

under the algebraic mapping

$$z = \frac{x}{x + L_{\mathrm{II}}}, \quad L_{\mathrm{II}} > 0. \tag{4.12}$$

Under the algebraic mapping (4.11), derivatives of the stream function $\psi_{\mathrm{I}}(x, y)$ with respect to x are transformed to derivatives with respect to z as

$$\frac{\partial^q \psi_{\mathrm{I}}}{\partial x^q} = \frac{1}{L_{\mathrm{I}}^q} \sum_{j=1}^{q} C_j^{(q)}(-1)^{q+j}(1-z)^{q+j} \frac{\partial^j \psi_{\mathrm{I}}}{\partial z^j}, \qquad q = 1, ..., 4, \tag{4.13}$$

and the coefficients $C_j^{(q)}$ can be found from the recurrence relation

$$(q + j)\, C_j^{(q)} + C_{j-1}^{(q)} = C_j^{(q+1)},$$

where

$$C_1^{(q)} = q!$$

A similar procedure is performed in region II for derivatives of ψ_{II}. The differential equation and interface continuity conditions are thus modified under the mappings (4.11) and (4.12).

In the transformed region M_{I} we seek an approximation to the stream function of the form

$$\psi_{\mathrm{I}}(z, y) = G_{\mathrm{I}}(y) + \sum_{m=0}^{M} \sum_{n=4}^{N} a_{mn} P_n(y)\, T_m^*(z),$$

and in region M_{II},

$$\psi_{\mathrm{II}}(z, y) = G_{\mathrm{II}}(y) + \sum_{m=0}^{L} \sum_{n=4}^{N} b_{mn} P_n(y/\alpha)\, T_m^*(z).$$

The collocation points are again chosen to be the extrema of the Chebyshev polynomial of highest degree used in the solution representations.

5. Numerical Results

5.1. *Chebyshev–Laguerre in Original Domain*

Results obtained using this approach were poor. The poor convergence was originally thought to be due to the choice of collocation points in the x-direction.

Therefore an idealized one-dimensional model problem was considered in order to diagnose the source of the difficulty. Consider the fourth-order linear differential equation

$$\frac{d^4u}{dx^4}+2\frac{d^2u}{dx^2}+\lambda^2 u=f(x), \qquad x\in[0,\infty), \tag{5.1}$$

with u and its first three derivatives prescribed at $x=0$ and λ a given constant. We seek an approximation to the solution $u(x)$ of (5.1) in the form of the weighted Laguerre representation

$$u_N(x)=e^{-\beta x}\sum_{n=0}^{N} a_n L_n(x). \tag{5.2}$$

The right-hand side, $f(x)$, is chosen so that the true solution of (5.1) has the form

$$u(x)=e^{-\alpha x}\cos\gamma x, \tag{5.3}$$

where α and γ are given constants chosen to correspond to the real and imaginary parts of the principal Papkovich–Fadle eigenvalue, respectively, i.e.,

$$\alpha=\lambda\simeq 3.749,$$

$$\gamma\simeq 2.769.$$

Numerical experiments were performed varying the value of β in (5.2). The results reveal that convergence is satisfactory only when the exponential mode of decay of the approximating function (5.2) is the same as that of the solution (5.3). In Table I the relative error in the computed solution is given at selected points for different values of β when $N=14$.

It is evident from the table that as we move further from the origin the relative accuracy degrades which is in accordance with remarks of Gottlieb and Orszag [9] concerning the accuracy of expansions of Laguerre polynomials. The sensitive region in the contraction problem is the area near the interface (origin) where the solutions in subregions I and II are matched. A significant observation from Table I, however, is that even near the origin the accuracy of the approximation degrades for different modes of decay to that of the solution. The study of the model problem (5.1) has thus been important in isolating the cause of the

TABLE I

Relative Errors at Selected Points for Different Values of β

x	$\beta=2.769$	$\beta=4.0$	$\beta=5.0$	$\beta=6.0$
0.0	0.3849 − 6	0.4094 − 5	0.1348 − 4	0.6581 − 4
0.2	0.5513 − 6	0.1985 − 5	0.3739 − 5	0.1167 − 3
0.4	0.4258 − 5	0.1026 − 4	0.8875 − 4	0.5684 − 3
0.6	0.1185 − 3	0.5684 − 3	0.5366 − 2	0.4474 − 1

difficulties associated with the contraction problem. Therefore a more sophisticated approach is necessary in order to obtain a more accurate representation of the solution.

5.2. *Chebyshev–Chebyshev in Truncated Domain*

In this approach numerical tests are performed with respect to the truncation lengths h_1 and h_2 in regions I and II, respectively. We consider the 4:1 ($\alpha = \frac{1}{4}$) and 2:1 ($\alpha = \frac{1}{2}$) contraction geometries. After extensive experimentation the best matched solutions were obtained with $h_1 = 2.0$ and $h_2 = 0.5$ for the 4:1 contraction and with $h_1 = 1.5$ and $h_2 = 0.5$ for the 2:1 contraction. Larger values of h_1 and h_2 correspond to a sparser distribution of collocation points in the neighbourhood of the interface. This results in degradation of the smoothness of the continuity between the elements and a poor description of the salient corner vortex. Smaller values of h_1 and h_2 lead to an inaccurate description of the far field flow since conditions (4.9) and (4.10) are imposed too close to the interface thereby not allowing sufficient entry and exit lengths to obtain a fully developed velocity profile.

A contour plot of the stream function for the 4:1 contraction is shown in Fig. 2a. This was obtained Chebyshev polynomial expansions of degree 16 in the y-direction in both elements and of degrees 16 and 8 in the x-direction in regions I and II,

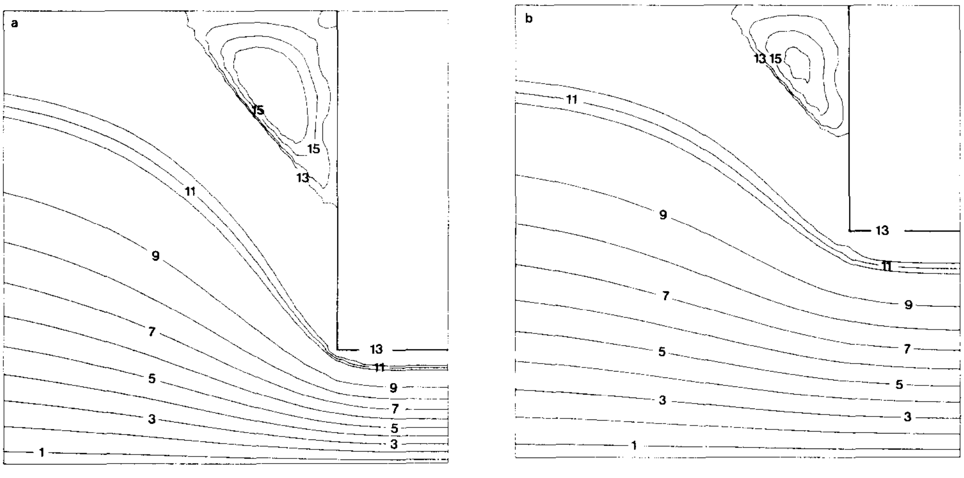

FIG. 2. (a) 4:1 contraction with $h_1 = 2.0$, $h_2 = 0.5$, $N = 16$, $M = 16$, $L = 8$; (b) 2:1 contraction with $h_1 = 1.5$, $h_2 = 0.5$, $N = 17$, $M = 14$, $L = 8$. Contour key:

1	0.0500	9	0.8500
2	0.1500	10	0.9500
3	0.2500	11	0.9600
4	0.3500	12	0.9700
5	0.4500	13	1.0000
6	0.5500	14	1.0001
7	0.6500	15	1.0003
8	0.7500	16	1.0005

respectively. The total number of degrees of freedom is therefore 338. A contour plot of the stream function for the 2:1 contraction is given in Fig. 2b. This was obtained using a comparable number of degrees of freedom to the 4:1 contraction.

The contour plot for the 4:1 contraction in Fig. 2a was compared with ones which had previously appeared in the literature for various degrees of freedom. For as few as 338 degrees of freedom we obtain results which are in qualitative agreement with those of Mendelson *et al.* [17] who use a finite element method with as many as 1326 degrees of freedom (92 elements). For the 2:1 contraction (see Fig. 2b) excellent agreement is observed with the results of Dennis and Smith [8] and Holstein and Paddon [11].

5.3. *Chebyshev–Chebyshev in Mapped Domain*

The results obtained using the algebraic mapping of the two semi-infinite elements onto finite rectangles are again satisfactory. For this case numerical tests are performed with respect to the mapping factors L_{I} and L_{II} in regions I and II, respectively. Large values of the mapping factors correspond to a sparse distribution of collocation points near the interface whereas small values correspond to a dense distribution there at the expense of a detailed description of the flow in the far field. The values of L_{I} and L_{II} which give the smoothest solution both across the interface and in the entry and exit sections are -2.0 and 0.5 for the 4:1 contraction and -1.8, and 0.6 for the 3:1 contraction.

In order to verify the convergence of the approximation we compare the solutions obtained with different numbers of degrees of freedom by increasing the degree of the approximating polynomial within each of the two elements. The transition from a low order approximating polynomial to a higher order one can be seen in Figs. 3a–d. The solution converges rapidly with the addition of only a small number of degrees of freedom at each stage. A contour plot of the stream function for the 3:1 contraction is given in Fig. 4 to validate the robustness of the present method.

The CPU times, in seconds, required to produce the results shown in Fig. 3 are tabulated in Table II for the various numbers of degrees of freedom. The computational effort is dominated by the need to invert large matrices which requires $O(K^3)$ operations where K denotes the size of the matrix, i.e., the total number of degrees

TABLE II

Variation of CPU Time with Number of Degrees of Freedom

N	M	L	Degrees of freedom	CPU time (s)
16	10	6	234	28.0
16	12	7	273	40.5
16	13	8	299	50.0
16	16	8	338	69.0

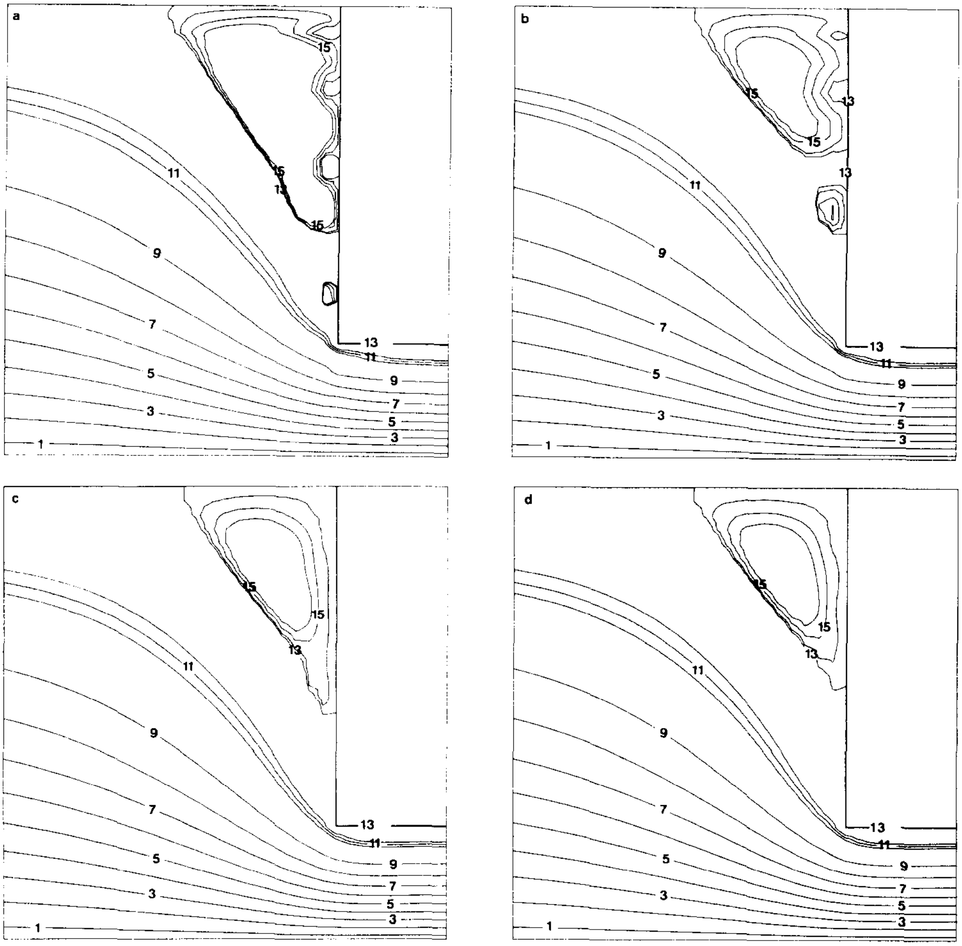

FIG. 3. 4:1 contraction with $L_{\mathrm{I}} = -2.0$, $L_{\mathrm{II}} = 0.5$: (a) $N = 16$, $M = 10$, $L = 6$ (234 degrees of freedom); (b) $N = 16$, $M = 12$, $L = 7$ (273 degrees of freedom); (c) $N = 16$, $M = 13$, $L = 8$ (299 degrees of freedom); (d) $N = 16$, $M = 16$, $L = 8$ (338 degrees of freedom). (see contour key for Fig. 2.)

of freedom. This is reflected in the way the CPU time increases with K. For a given number of degrees of freedom this means that the spectral collocation method considered here is more expensive than conventional finite difference methods. However, far fewer degrees of freedom are required in a spectral representation than a finite difference one to attain comparable accuracy (see, e.g., [8]). The computations were performed on a CDC 7600 computer located at the University of Manchester.

Further increasing the number of degrees of freedom beyond the number used to produce Fig. 3d had no visible effect on the stream function contours. The appearance of miniature eddies at the corner (0, 1) in Figs. 2a and 4 is possibly a result of the presence of weak singularities there (see [18]).

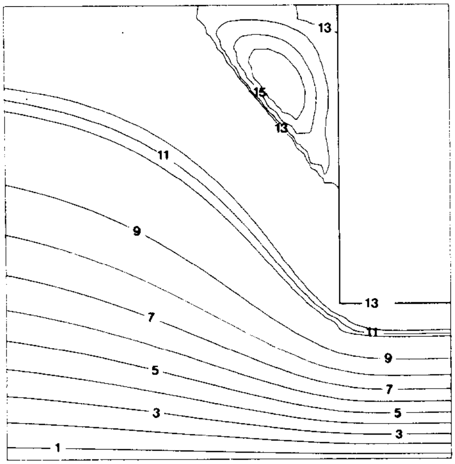

FIG. 4. 3:1 contraction with $L_{\rm I} = -1.8$, $L_{\rm II} = 0.6$, $N = 16$, $M = 16$, $L = 8$. (See contour key for Fig. 2.)

6. CONCLUSIONS

The present study investigates Stokes flow in contraction geometries and unbounded domains. A spectral element method is presented which solves the governing equation of motion for the stream function as a set of coupled problems over semi-infinite rectangular subregions or elements. The solutions in the two elements are matched by imposing C^3 interface continuity conditions in the collocation sense. Several choices or trial functions are considered.

An attempt to approximate the solution by a weighted Laguerre–Chebyshev expansion failed since it did not represent the exponential rate of decay of the solution at entry and exit. A conventional domain truncation technique produced satisfactory results with far fewer degrees of freedom than are required for finite difference and finite element solutions. However, these truncation methods are really only adequate for treating the flow of fluids which possess no memory, i.e., Newtonian fluids. This is because when elastic effects dominate, the entry and exit lengths need to be extended considerably in order to obtain a fully developed velocity profile. To overcome this we propose the use of algebraic mapping techniques which involves mapping the two semi-infinite regions of the problem onto two finite rectangles. This approach proved to be extremely promising.

The underlying structure of the linear system of algebraic equations has not yet been fully exploited. If this were done then considerable reductions in the amount of computer storage required would be achieved. Alternatives to the direct methods of solution used in the present paper taking advantage of the block tridiagonal structure of the spectral element matrix are currently under investigation.

The techniques developed in Karageorghis, Phillips, and Davies [13] and the present paper now provide the framework within which the non-Newtonian problem can be tackled.

Acknowledgments

The authors are grateful to the UK Science and Engineering Research Council for financial support which enabled this work to be performed. We also record our thanks to Dr. A. R. Davies for many enlightening discussions.

References

1. J. P. Boyd, *J. Comput. Phys.* **45**, 43 (1982).
2. C. J. Coleman, *Q. J. Mech. Appl. Math.* **34**, 453 (1981).
3. C. J. Coleman, *J. Non-Newtonian Fluid Mech.* **15**, 227 (1984).
4. M. J. Crochet, A. R. Davies and K. Walters, *Numerical Simulation of Non-Newtonian Flow* (Elsevier, Amsterdam, 1984).
5. A. R. Davies, "Reentrant Corner Singularities in Non-Newtonian Flow," Fifth Workshop on Numerical Methods in non-Newtonian Flow, Lake Arrowhead, California, June 1987.
6. A. R. Davies, A. Karageorghis, and T. N. Phillips, *Int. J. Num. Methods Eng.* **26**, 647 (1988).
7. L. M. Delves and C. A. Hall, *J. Inst. Math. Appl.* **23**, 223 (1979).
8. S. C. R. Dennis and F. T. Smith, *Proc. R. Soc. London A* **372**, 393 (1980).
9. D. Gottlieb and S. A. Orszag, *Numerical Analysis of Spectral Methods: Theory and Applications*, CBMS-NSF Regional Conference Series in Applied Mathematics Vol. 26 (SIAM, Philadelphia, 1977).
10. C. E. Grosch and S. A. Orszag, *J. Comput. Phys.* **25**, 273 (1977).
11. H. Holstein and D. J. Paddon, in *Numerical Methods for Fluid Dynamics*, edited by K. W. Morton and M. J. Baines (Academic Press, New York, 1982), p. 341.
12. D. D. Joseph, *J. Non-Newtonian Fluid Mech.* **10**, 185 (1982).
13. A. Karageorghis, T. N. Phillips, and A. R. Davies, *Int. J. Numer. Meth. Eng.* **26**, 805 (1988).
14. Y. Maday, B. Pernaud-Thomas, and H. Vandeven, *Rech. Aerosp.* **6**, 353 (1985).
15. C. Mivriplis, Laguerre polynomials for infinite-domain spectral elements, *J. Comput. Phys.*, in press.
16. J. M. Marchal and M. J. Crochet, *J. Non-Newtonian Fluid Mech.* **20**, 187 (1986).
17. M. A. Mendelson, P. W. Veh, R. A. Brown, and R. C. Armstrong, *J. Non-Newtonian Fluid Mech.* **10**, 31 (1982).
18. H. K. Moffatt, *J. Fluid. Mech.* **18**, 1 (1964).
19. Y. Morchoisne, in *Spectral Methods for Partial Differential Equations*, edited by R. G. Voigt, D. Gottlieb, and M. Y. Hussaini (SIAM, Philadelphia, 1984), p. 181.
20. S. A. Orszag, *J. Comput. Phys.* **37**, 70 (1980).
21. A. T. Patera, *J. Comput. Phys.* **54**, 468 (1984).
22. T. N. Phillips and A. R. Davies, *J. Comput. Appl. Math.* **21**, 173 (1988).
23. G. Sansone, *Orthogonal Functions* (Krieger, New York, 1977).
24. F. Thomasset, *Implementation of Finite Element Methods for Navier–Stokes Equations* (Springer-Verlag, New York, 1981).